Available online at www.sciencedirect.com
SCIENCE DIRECT®
Mechanics of Materials 37 (2005) 261–273
MECHANICS OF MATERIALS
www.elsevier.com/locate/mechmat

Delocalizing strain in a thin metal film on a polymer substrate

T. Li [a], Z.Y. Huang [a], Z.C. Xi [b], S.P. Lacour [c], S. Wagner [c], Z. Suo [a,*]

[a] Division of Engineering and Applied Sciences, Harvard University, Cambridge, MA 02138, USA
[b] Center for Composite Materials, University of Delaware, Newark, DE 19716, USA
[c] Department of Electrical Engineering, Princeton University, Princeton, NJ 08544, USA

Received 10 June 2003; received in revised form 28 January 2004

Abstract

Under tension, a freestanding thin metal film usually ruptures at a smaller strain than its bulk counterpart. Often this apparent brittleness does not result from cleavage, but from strain localization, such as necking. By volume conservation, necking causes local elongation. This elongation is much smaller than the film length, and adds little to the overall strain. The film ruptures when the overall strain just exceeds the necking initiation strain, ε_N, which for a weakly hardening film is not far beyond its elastic limit. Now consider a weakly hardening metal film on a steeply hardening polymer substrate. If the metal film is fully bonded to the polymer substrate, the substrate suppresses large local elongation in the film, so that the metal film may deform uniformly far beyond ε_N. If the metal film debonds from the substrate, however, the film becomes freestanding and ruptures at a smaller strain than the fully bonded film; the polymer substrate remains intact. We study strain delocalization in the metal film on the polymer substrate by analyzing incipient and large-amplitude nonuniform deformation, as well as debond-assisted necking. The theoretical considerations call for further experiments to clarify the rupture behavior of the metal-on-polymer laminates.

1. Introduction

Deformable electronics have diverse applications, such as curved imaging surfaces (Hsu et al., 2002), sensor skins (Gleskova et al., 1999), and electronic textiles (Lumelsky et al., 2001; Wagner et al., 2002). One way to make a deformable device is to start with a polymer substrate, fabricate on the substrate small islands with a stiff material (e.g., silicon nitride), and place on the islands all brittle components (e.g., silicon and silicon dioxide). When the structure is stretched, strains are small in the islands and in the brittle components, but large in parts of the polymer substrate left uncovered by the islands. Metal films, deposited on the polymer substrate to connect the islands, must deform with the substrate.

* Corresponding author. Tel.: +1 617 4953789; fax: +1 617 4960601.
E-mail address: suo@deas.harvard.edu (Z. Suo).

0167-6636/$ - see front matter © 2004 Elsevier Ltd. All rights reserved.
doi:10.1016/j.mechmat.2004.02.002

A key question is whether the metal films can survive large strains without rupture. The same question has been asked for metal–polymer laminates widely used for electronic and food packaging (Merchant et al., 2000).

The present paper considers this question for an idealized structure: a blanket metal film bonded to a polymer substrate, subject to a tensile strain in the plane of the film (Fig. 1). Attention is restricted to metal films that rupture by strain localization (e.g., necking or forming a shear band). Strain localization causes a large local elongation in the metal film, which cannot be accommodated by the polymer substrate subject to a modest strain. One therefore expects that, substrate-bonded and strain delocalized, the metal film may deform uniformly far beyond when strain localization would occur if the film were freestanding. Of course, substrate constraint disappears if the metal film debonds from the polymer substrate. When the laminate is subject to a modest tensile strain, we expect strain localization and debond to co-evolve. Without debonding, the polymer substrate suppresses strain localization in the metal. Without localization, no traction exists on the interface to drive debonding. The conundrum parallels that of buckle-debond co-evolution of a compressive film on a substrate (Hutchinson and Suo, 1992).

As will be discussed, the experimental evidence available to us is suggestive, but insufficient to fully confirm these expectations. To plan systematic experiments, this paper integrates theoretical aspects of thin film rupture. Section 2 reviews experimental observations of both freestanding and substrate-bonded films under tension, and collects elementary considerations that are independent of the detailed plasticity theory. Guided by these considerations, we will use the continuum plasticity theory in the subsequent analysis. Section 3 studies the incipient nonuniform deformation using a linear perturbation analysis. The analysis shows that the substrate greatly elevates the applied strains needed for long wave perturbations to amplify. The linear perturbation analysis, however, is invalid when the perturbation amplitude is comparable to the film thickness, or the perturbation wavelength, or the material inhomogeneity size. To address these concerns, Section 4 studies large-amplitude nonuniform deformation using the finite element method. Section 5 studies debond-assisted necking, also using the finite element method.

2. Strain localization and delocalization

Compared to bulk metals, freestanding thin metal films usually have high strengths, but small rupture strains (Pashley, 1960; Xiang et al., 2002; Espinosa et al., 2003; Lee et al., 2003; Baral et al., 1984; Keller et al., 1996; Huang and Spaepen, 2000). For example, Pashley (1960) reported experiments with single-crystal gold films, 50–200 nm thick, stretched in the transmission electron microscope. The films deformed elastically to about 1% strain and ruptured. Nonetheless Pash-

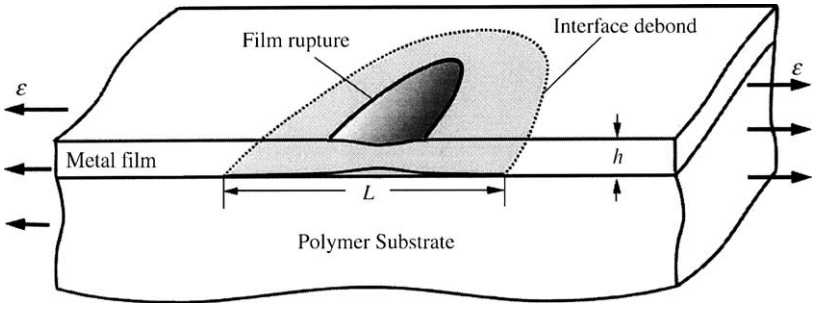

Fig. 1. A metal film is initially bonded to a thick polymer substrate. Subject to a tensile strain in the plane of the film, the film rupture and the interface debond co-evolve. The rupture occurs by localized strain in a segment of the film, of length comparable to the film thickness, but debond spreads over a segment of the interface many times the film thickness.

ley observed dislocation activities and local thinning. The experimental findings have been interpreted as follows. The large elastic limit in a thin metal film results from the difficulty in operating dislocation sources. Upon initiation, dislocations move across the film and escape from the surfaces. The film strains plastically, but does not harden. Local thinning raises local stresses. Without hardening, subsequent thinning localizes in a segment of the film, of length comparable to the film thickness, leading to rupture. The total length of the film is much larger than its thickness, so that the apparent rupture strain is just slightly beyond its the elastic limit. In Pashley's own words, "The fracture of the single-crystal gold films is in no sense brittle, but results from localized deformation".

A freestanding polycrystalline thin metal film may strain somewhat beyond the elastic limit (Xiang et al., 2002; Espinosa et al., 2003). Dislocations pile up at grain boundaries, and harden the film. Strain localization has also been observed in polycrystalline copper and aluminum films (Espinosa et al., 2003; Lee et al., 2003). The analysis in the subsequent sections will assume that the metal film hardens weakly, such that the necking strain for the freestanding film, ε_N is only slightly larger than the elastic limit strain.

The invisible ductility can be made visible. Fig. 2 compares the freestanding and the substrate-bonded films. At the site of rupture, strain localization causes a large local elongation on the order of the film thickness. The local elongation requires space to accommodate. This space is available to the freestanding film, but unavailable to the substrate-bonded film subject to a modest tensile strain. Consequently, the polymer substrate may delocalize deformation in the metal film, carrying the metal film to strains far beyond its necking limit without rupture. Fig. 2 illustrates strain localization by necking, but similar arguments apply to localization by forming a shear band.

This geometric constraint is further appreciated by considering a film of an intrinsically brittle material (such as silicon nitride) that ruptures by cleavage (Fig. 3). In this case, rupture involves breaking a single array of atomic bonds: no large local elongation occurs. Consequently, the presence of the polymer substrate does little to prevent the film from cleavage. (The presence of the substrate does reduce the driving force on a long channel crack by limiting the opening in its wake.)

Now return to rupture by strain localization. When the metal film debonds from the polymer substrate, the film becomes freestanding. The debond length, L, serves as the gauge length in the tensile test, so long as the polymer is sufficiently stiff. As the film approaches rupture, the local thinning gives a local elongation of magnitude proportional to the film thickness, h. The rest of the film is strained to the level approximately of the necking strain of an infinitely long freestanding film, ε_N. Consequently, when the partially debonded film

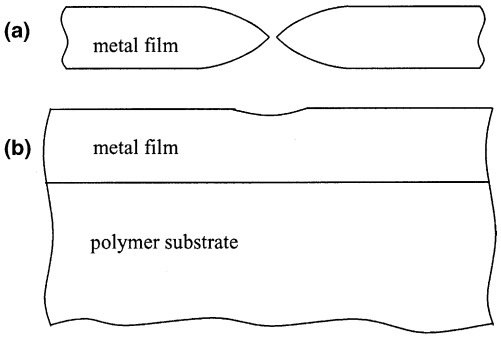

Fig. 2. When rupture is caused by strain localization, local thinning leads to local elongation. (a) For a freestanding metal film, the local elongation is accommodated by rigid body motion of the ruptured halves. (b) For a substrate-bonded film, the local elongation may be suppressed by the substrate.

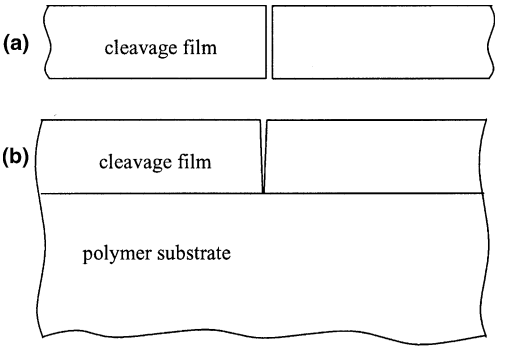

Fig. 3. When rupture is caused by cleavage, breaking a single array of atomic bonds, no local elongation is involved. The presence of the substrate does little to suppress rupture.

ruptures, the applied strain, estimated by the net elongation of the debonded film divided by the debond length is

$$\varepsilon \approx \varepsilon_N + \alpha h/L, \tag{1}$$

where α is a dimensionless number of order unity. The larger the debond length, the smaller the rupture strain. To knock down the rupture strain to the order of a few percent, the debond length has to be about 100 times the film thickness.

Many tensile experiments have been reported for metal films on polymer substrates. Hommel and Kraft (2001) deformed Cu films on a polyimide substrate up to 2% strains, but did not report any rupture behavior. Similar studies have been carried out by Kraft et al. (2000), and by Yu and Spaepen (2004). The latter also provides a bibliography of earlier literature on the subject. Several groups have reported rupture behavior of metal films on polymer substrates (Gage and Phanitsiri, 2001; Chiu et al., 1994; Alaca et al., 2002). When the metal–polymer laminates are subject to larger strains, parallel cracks, of spacing much larger than the film thickness, run through the metal films. The polymer substrates remain intact. As the strain increased, more and more cracks form. Metal–polymer debonding is observed. Kang (1996) reported that some of his aluminum films, bonded on a polyimide substrate, did not form any crack after a strain of 20%. Lacour et al. (2003) studied gold films on an elastomer substrate. At about 8% strain, small cracks appeared at the edges of the film but did not propagate far into the film. The gold film remained electrically conductive up to a strain of 23%. Under large tensile strains, the film wrinkles in the direction perpendicular to the loading direction. More recent work suggested that, in this particular experiment, the gold grains may have functioned like loosely linked islands (Lacour, private communication).

For a metal film on a substrate, the interface may block dislocation motion and lead to steep hardening, as observed under small strains in wafer bending experiments (Nix, 1998), and in a numerical simulation that assumes a hard interface (Nicola et al., 2003). However, experimental evidence is lacking for substrate-bonded films hardening at large strains. A dislocation impinging on the metal–polymer interface may escape by spreading the core along the interface (Baker et al., 2002). To be conservative, the following analysis neglects the interfacial contribution to hardening.

Guided by the above considerations, the next three sections will study the conditions for strain localization using a conventional continuum plasticity theory. Such a theory has been under attacks on multiple fronts, but we will not invoke more sophisticated theories or computational schemes in this work, for the phenomenon under study is largely geometrical.

Under the uniaxial stress state, the true stress σ and the natural strain ε are taken to obey the power law

$$\sigma = K\varepsilon^N. \tag{2}$$

The two constants N (the hardening index) and K are material specific. This relation is extended to multiaxial stress states according to the J_2-deformation theory. We will model both the metal and the polymer with the power law stress–strain relation, with $N=0.02$ and $K=114$ MPa for the metal, and $N=0.5$ and $K=632$ MPa for the polymer. These values are representative of a weakly hardening metal and a strong, steeply hardening polymer (e.g., a polyimide). Fig. 4 compares the stress–strain curves for the two model materials. At small strains, the metal carries higher stresses

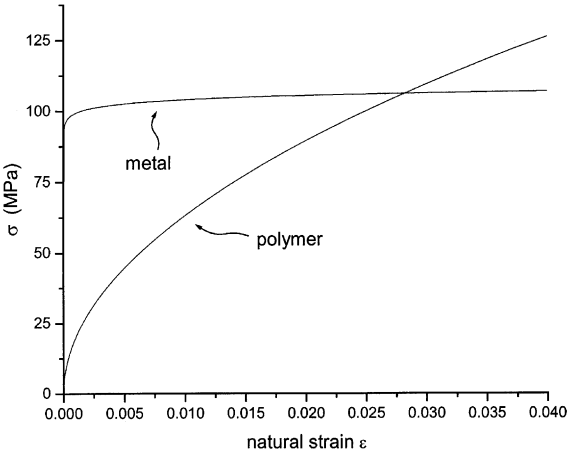

Fig. 4. The stress–strain curves for a weakly hardening metal and a steeply hardening polymer.

than the polymer. As the strain increases, the stress increases slightly in the metal, but steeply in the polymer.

3. Incipient nonuniform deformation

When the applied strain is small, the laminate deforms uniformly. When the applied strain is large, nonuniform deformation develops. The bifurcation problem has been studied extensively (e.g., Hill and Hutchinson, 1975; Stören and Rice, 1975; Dorris and Nemat-Nasser, 1980; Steif, 1986; Bigoni et al., 1997). This section gathers results useful to our discussion.

Let the coordinate plane (x_1, x_2) coincide with a surface of the film, and the coordinate x_2 with the thickness direction of the film. For simplicity, we assume that the laminate deforms under the plane strain conditions in the plane (x_1, x_3). The applied tensile strain is along the x_1 direction, of magnitude ε. In the linear perturbation analysis, the perturbation from the uniform state is taken to be sinusoidal in x_1, with the wave number k and the wavelength $2\pi/k$. The bifurcation strain depends on the wave number.

First consider a freestanding layer of thickness h. In the long wave limit, $kh \to 0$, the field varies slowly along x_1. Consequently, one can think of the layer as a series of segments, each having a uniform strain. Different segments can have different strain levels but must carry the same force. The well-known elementary Considere calculation shows that the uniform deformation is unstable when the strain reaches

$$\varepsilon = N. \tag{3}$$

This strain is taken to be the necking limit for a freestanding film, ε_N.

In the short wave limit, $kh \to \infty$, when the perturbation wavelength is much shorter than the layer thickness, the nonuniform deformation develops near the surfaces of the layer, and decays exponentially in the thickness direction of the layer. The situation is analogous to the Rayleigh wave. The bifurcation strain is determined by the equation

$$\varepsilon - \varepsilon \exp(-2\varepsilon) - N = 0. \tag{4}$$

For small N, the bifurcation strain for the surface mode is $\varepsilon \approx \sqrt{N/2}$.

The material loses ellipticity at an even higher strain. When the applied strain exceeds the ellipticity limit, the layer is in the hyperbolic regime, and can form shear bands. The situation is analogous to the body wave. The strain of the ellipticity limit is independent of the wave number, and is determined by the equation

$$(\varepsilon - N)^2 - \frac{4N\varepsilon}{\exp(4\varepsilon) - 1} = 0. \tag{5}$$

For small N, the ellipticity limit is $\varepsilon \approx \sqrt{N}$.

Fig. 5 plots Eqs. (3)–(5), showing the three critical strains as functions of the hardening index. For our model metal ($N = 0.02$), the strain is 0.02 for the long wave limit, 0.105 for the surface mode, and 0.142 for the ellipticity limit. For our model polymer ($N = 0.50$), the strain is 0.50 for the long wave limit, 0.675 for the surface mode, and 0.772 for the ellipticity limit. Because the polymer strain-hardens more steeply than the metal, all critical strains are higher for the polymer than their counterparts for the metal.

Fig. 6 plots the critical strain as a function of the wave number for a freestanding metal film ($N = 0.02$). The plot depends only on the hardening index N. The ellipticity limit is the horizontal line $\varepsilon = 0.142$, above which the film is in the hyperbolic

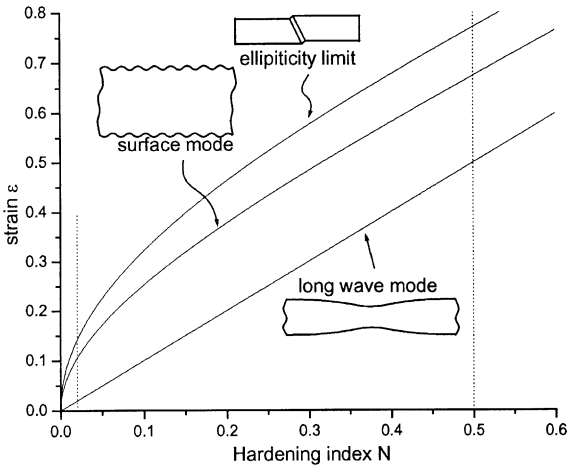

Fig. 5. Various critical strains as functions of the hardening index for a freestanding layer.

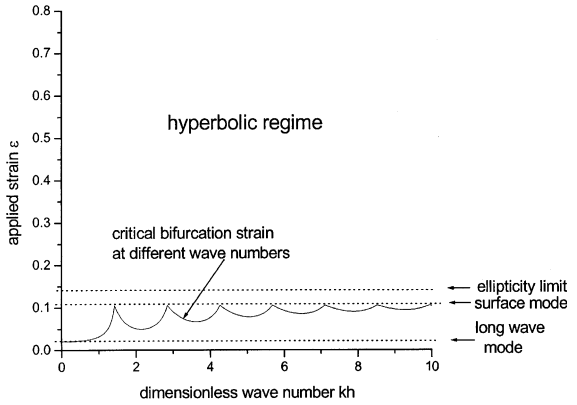

Fig. 6. The critical strain as a function of the wave number for the freestanding metal film.

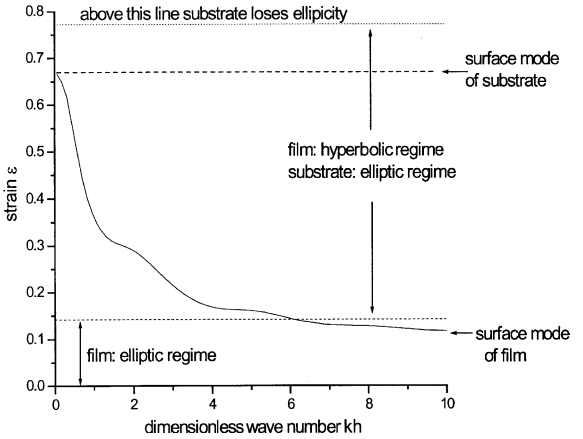

Fig. 7. The critical strain as a function of the wave number for the metal-on-polymer.

regime. The curve approaches the long wave limit $\varepsilon = 0.02$ and the short wave limit $\varepsilon = 0.105$. The wavy shape in between is determined from an eigenvalue equation (Hill and Hutchinson, 1975).

We next consider a thin metal film bonded to a polymer substrate. For simplicity, we assume that the thickness of the polymer substrate is infinite, i.e., much larger than the film thickness and the wavelengths under consideration. When the applied strain is small, the laminate deforms uniformly. When the applied strain is large, the nonuniform deformation develops, mainly in the metal film and near the substrate surface. The situation is analogous to the Lame wave. We determine the bifurcation strain using the same procedure in as the literature (Dorris and Nemat-Nasser, 1980; Steif, 1986; Bigoni et al., 1997). Fig. 7 plots the bifurcation strain as a function of the wave number. This plot depends on three dimensionless parameters: the hardening index for the metal (0.02), the hardening index for the polymer (0.5), and the ratio of the K values of the two materials (114/632).

The main features of Fig. 7 are readily understood. When the wavelength is large compared to the film thickness ($kh \to 0$), the metal film is negligible, and the critical strain corresponds to that of the surface mode for the freestanding polymer. When the wavelength is small compared to the film thickness ($kh \to \infty$), the polymer substrate is unimportant, and the critical strain corresponds to that of the surface mode for the freestanding metal. Even when the strain exceeds the ellipticity limit of the film, displacement continuity at the interface suppresses the localized shear band, and the perturbation is still sinusoidal.

A comparison of Figs. 6 and 7 gives some impression of the substrate effect. At long wavelengths ($kh \to 0$), the polymer substrate greatly elevates the critical strain above that for the freestanding film. One should also expect that the linear perturbation analysis is reliable for long wavelength perturbations, where the size scale of the geometric and material heterogeneities in the film are small compared to the wavelengths, and should not significantly affect the results much. At short wavelengths ($kh \to \infty$), however, the presence of the polymer substrate does not affect the critical strain.

4. Large-amplitude nonuniform deformation

The last prediction of the linear perturbation analysis raises the concern that the substrate may not suppress strain localization. This may be particularly alarming if the metal film does not harden at all, in which case the bifurcation strain for the surface mode of the metal is negligibly small. This concern is unjustified. For rupture to occur at short wavelengths at a modest applied strain, large

strains must occur locally. The linear stability analysis fails when the amplitude of the nonuniform displacement is large compared to the wavelength.

We next use the finite element code ABAQUS to simulate large-amplitude nonuniform deformation in both freestanding and substrate-bonded metal films. The imperfections are prescribed by perturbing the film top surface into a sinusoidal shape of amplitude $h/100$. We simulate deformation of two wave modes: a short wave ($kh = 10\pi$) and a long wave ($kh = \pi/5$). The subsequent deformation will be nonsinusoidal, and can have large amplitude. The finite element models are two wavelengths long. The substrate, if present, is 40 times the film thickness. The displacement is set to zero at the left-bottom corner of the models, so is the horizontal displacement along the left end of the models. Displacement in the horizontal direction, u, is prescribed along the right end of the models. Shear stress is prescribed to be zero at both ends of the model. In describing the results, we call the quantity $\ln(1 + u/l_0)$ the applied strain, where l_0 is the initial length of the models. Four-node quadrilateral plane strain elements are used everywhere. The film has 10 layers of elements in the thickness direction and a comparable element size in the in-plane direction. Matching elements are used along the interface between the film and the substrate. Coarser elements are used in the part of substrate far away from the interface.

Fig. 8 shows the deformation sequence of the freestanding film in the short wave mode ($kh = 10\pi$). The perturbation amplitude on the top surface starts to grow appreciably after the applied strain exceeds the bifurcation strain at the wavelength, 0.1, and increases to about twice its initial value at $\varepsilon = 0.11$. The perturbation also propagates across the film thickness to its bottom surface. The perturbation amplitudes on both surfaces reach about two times the initial amplitude when the applied strain is 0.18, and change very little as the applied strain further increases.

Fig. 9 shows the deformation sequence of the freestanding film in the long wave mode ($kh = \pi/5$). The perturbation amplitude does not change much at $\varepsilon = 0.01$. However, as the long wavelength bifurcation strain is approached, at $\varepsilon = 0.018$, the perturbation amplifies at the troughs, and propagates to the bottom film surface. Increasing applied strain causes thinning at the troughs. Rupture occurs at a strain around $\varepsilon = 0.023$. The results qualitatively agree with those of an earlier calculation (Tvergaard et al., 1981).

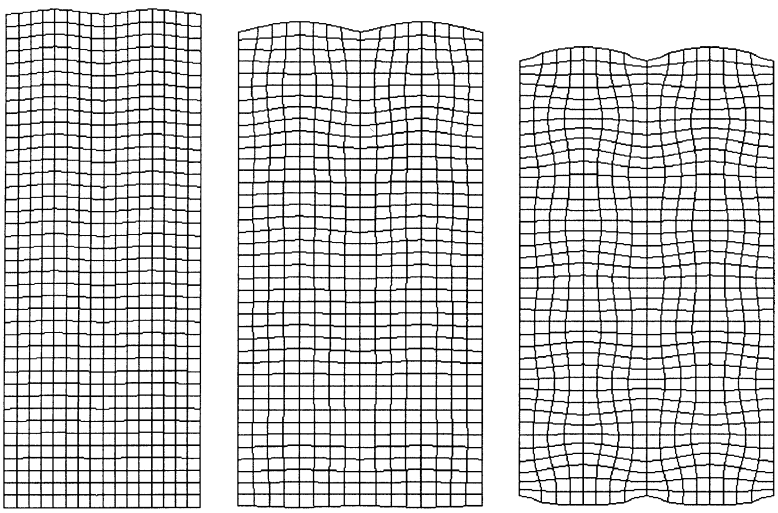

Fig. 8. Deformed meshes of a freestanding thin film with sinusoidal perturbation of a short wavelength on top surface under applied tensile strain. Initial wave number of the perturbation, $kh = 10\pi$.

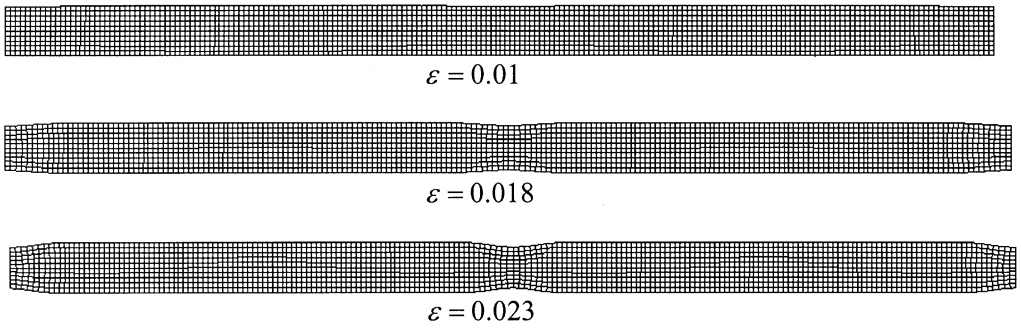

Fig. 9. Deformed meshes of a freestanding thin film with sinusoidal perturbation of a long wavelength on top surface under applied tensile strain. Initial wave number of the perturbation, $kh = \pi/5$.

In both short and long wave modes, the perturbation on the top film surface propagates to the bottom surface. As predicted by linear perturbation analysis, the short wave perturbation starts to grow at the bifurcation strain of 0.105, but the growth is stable and the film can sustain much lar-

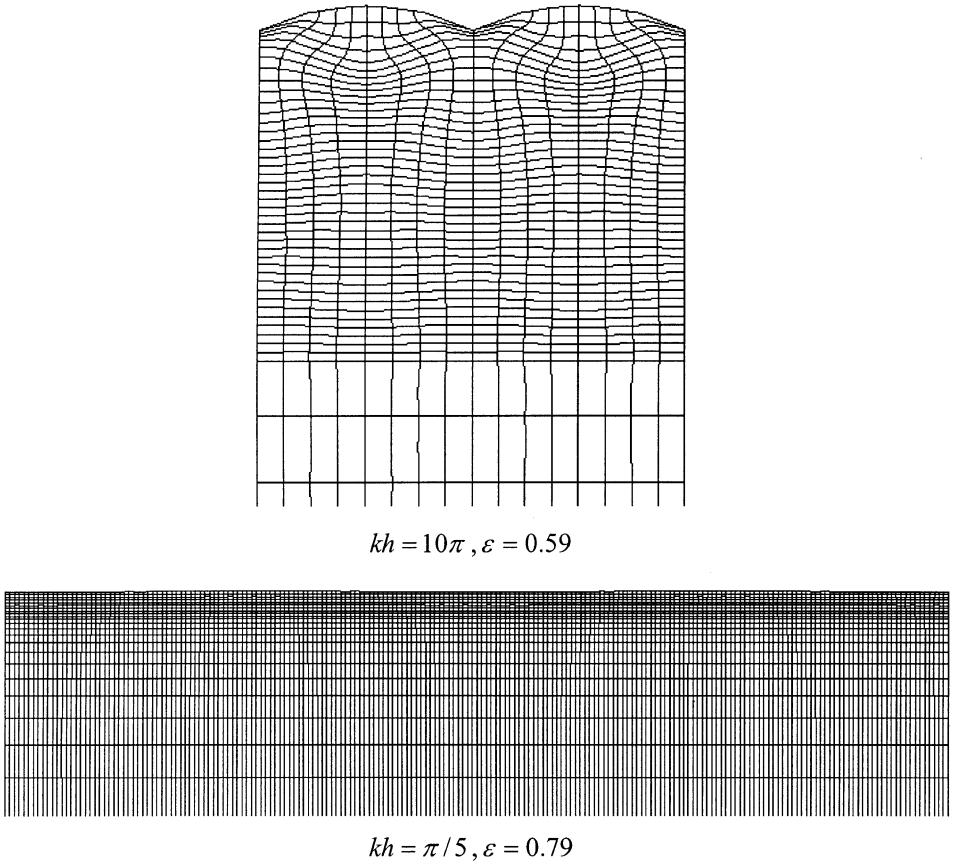

Fig. 10. Deformed meshes of a fully bonded metal-on-polymer under applied tensile strain. Nonuniform deformation of two wavelengths is simulated. In both cases, the substrate delocalizes strain in the metal film.

ger strains without rupture. On the other hand, the long wave perturbation localizes at the trough and lead to rupture soon after the bifurcation strain is exceeded.

We next discuss metal films bonded to the polymer substrate. Fig. 10 shows the meshes for the short and the long wave modes. For the short wave mode, the perturbation amplitude on the free surface of the film starts to grow at an applied strain of around 0.10, which agrees with the prediction of the linear perturbation analysis. However, the substrate prevents the perturbation from propagating from the free surface to the interface. For the long wave mode, even the amplitude of the perturbation does not increase appreciably under large applied strains. The finite element simulation shows that the substrate suppresses large-amplitude nonuniform deformation for both short and long wavelengths.

5. Debond-assisted necking

Upon debonding from the substrate, the film becomes freestanding. As pointed out before, debonding and strain localization will progress simultaneously. The debond length will depend on the adhesion between the metal and the polymer, as well as the stress–strain relations of the two materials. A full understanding would require that debond and strain localization be analyzed as a coupled problem, in three dimensions. In this section, we will consider a simpler problem. We will specify the debond length, and investigate its effect on rupture.

A V-shaped imperfection is introduced at the center of the top surface of the film such that the film thickness at the center is $0.99h$. Debond is introduced at the central part of the interface. Due to symmetry, the finite element model only takes the right half of the structure. The width of the whole structure is $40h$. Two cases are calculated: a short debond length $L=4h$, and a long debond length $L=20h$.

Fig. 11 shows the deformation sequence of the laminate with the short debond length. Strain localization begins at an applied strain of 0.04, and grows as the applied strain increases. Rupture occurs at an applied strain of 0.13. Fig. 12 shows the deformation sequence of the laminate with the long debond length. The thin film starts to neck at an applied tensile strain smaller than that in the shorter debonding length case, and rupture occurs at a strain of about 0.05. The simple estimation of Eq. (1) gives the rupture strains $\varepsilon=0.27$ for $L=4h$, and $\varepsilon=0.07$ for $L=20h$. The estimates agree with the FEM results within 50%. Eq. (1) neglects the compliance of the polymer around the debond front, and therefore overestimates the effect of the substrate constraint on film rupture.

FEM results indicate that the debond length has considerable impact on the rupture strain. The longer the debond length, the smaller the rupture strain. The large local elongation at rupture is mainly accommodated by the debonded part of the thin film. For a short debond length, a large applied strain is required to accommodate the local elongation. For a long debond length, a small applied strain can accommodate the local elongation.

As necking develops, the debonded film separates from the substrate. This is due to the asymmetry of the structure in the thickness direction. More lateral separation provides more space to accommodate the large local elongation at necking. The necking-induced interfacial opening also generates the driving force for further debonding.

Additional FEM calculation for a polymer with hardening index $N=0.1$ shows lower rupture strains. The larger the hardening index, the higher the rupture strain. This is because the large local elongation is accommodated not only by the thin film and lateral separation, but also by the deformation of the substrate. This becomes more evident at large applied tensile strains, where the substrate is hardened to a great extent. The higher hardening index indicates that a higher stress level for the substrate is required to conform to the thin film deformation, which corresponds to a higher rupture strain for the film.

6. Concluding remarks

Freestanding or substrate-bonded, thin metal films may rupture by strain localization, rather than by cleavage. A freestanding metal film

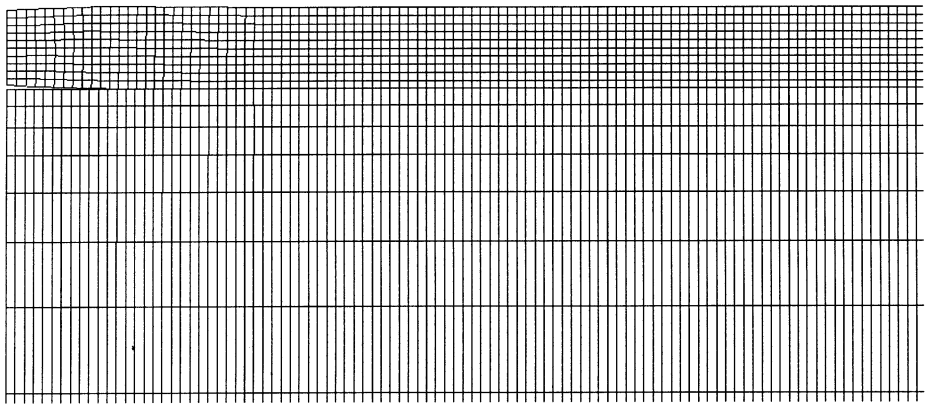

$\varepsilon = 0.04$

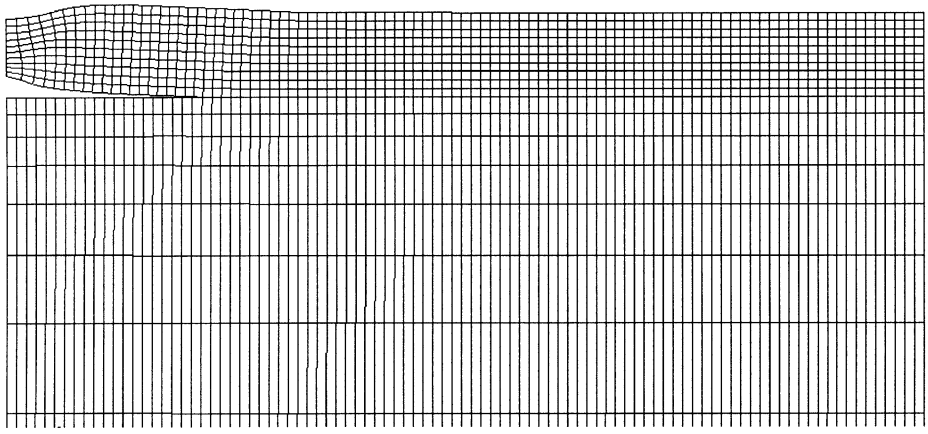

$\varepsilon = 0.08$

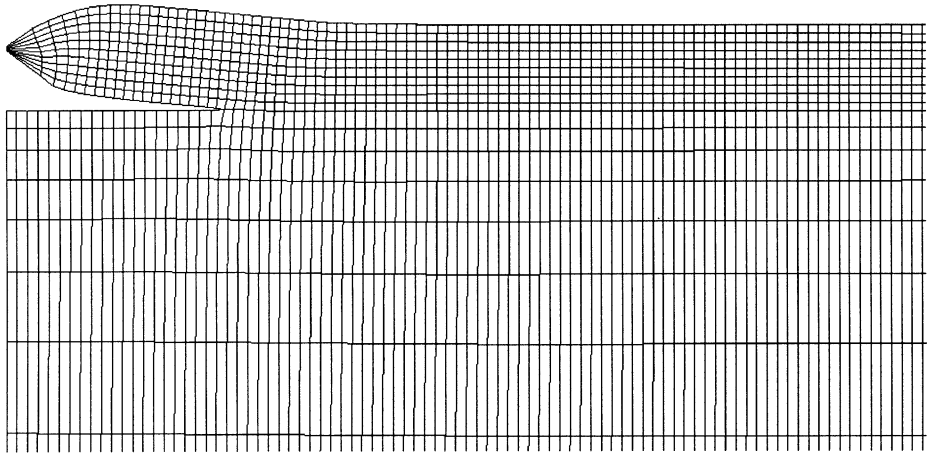

$\varepsilon = 0.13$

Fig. 11. Deformation sequence of a film partially debonded from the substrate (debond length $L = 4h$).

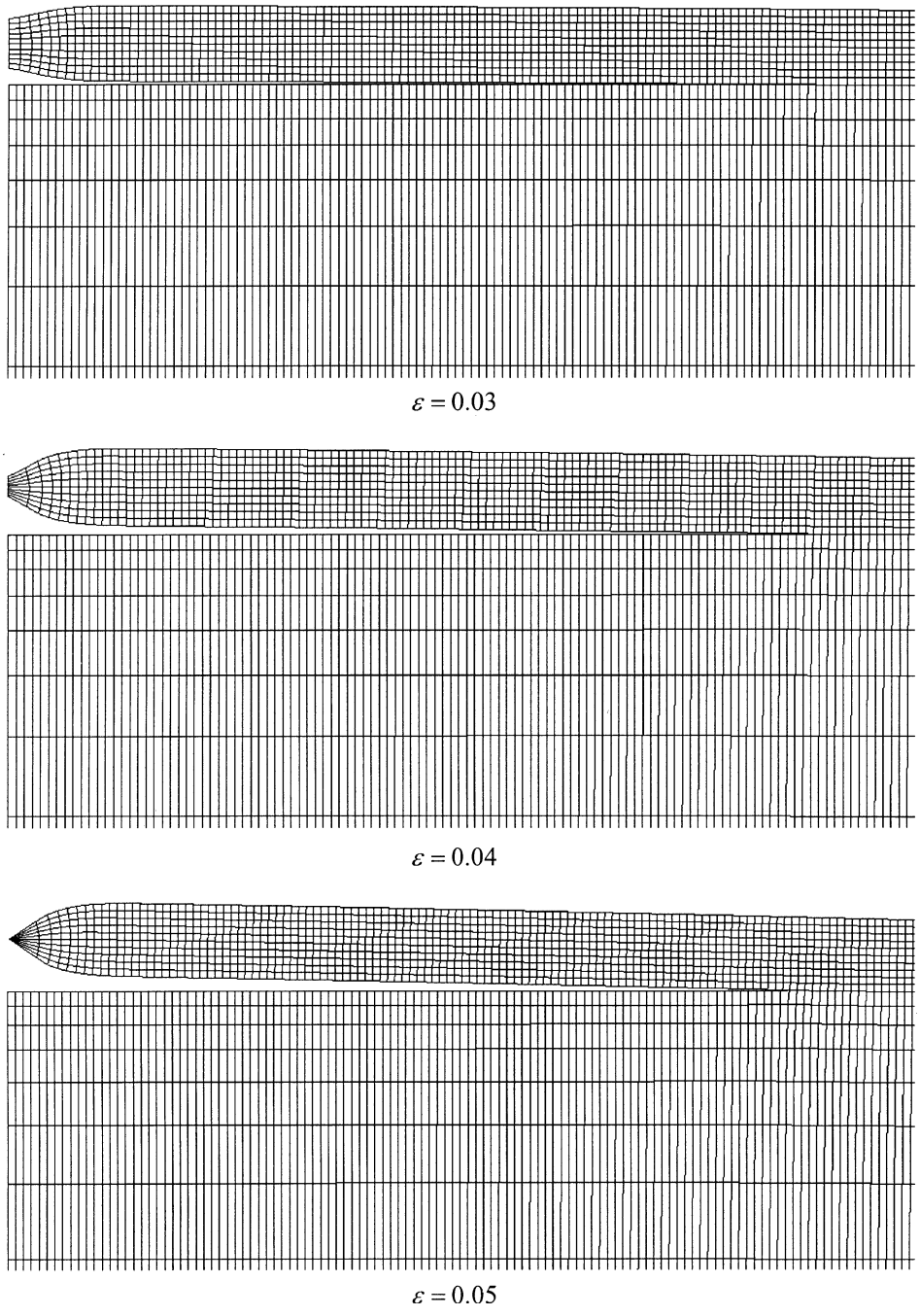

Fig. 12. Deformation sequence of a film partially debonded from the substrate (debond length $L = 20h$).

accommodates the local elongation by rigid body motion of the ruptured halves. A substrate-bonded metal film cannot have large local elongation, and may therefore deform uniformly far beyond the elastic limit. The support of the substrate is lost if the film debonds from the substrate. We analyze

a weakly hardening metal film on a strong, steeply hardening polymer substrate. The linear perturbation analysis shows that the presence of the substrate elevates the bifurcation strain for long wave perturbations, but does not affect that for short wave perturbations. The finite element analysis shows that large strains are needed to significantly amplify the short wave perturbations. Together, these two analyses show that the weakly hardening metal film, fully bonded to the steeply hardening polymer substrate, can sustain large strains against perturbations of all wavelengths. Finite element analysis is also used to study debond-assisted necking. As expected, the longer the debond length, the smaller the rupture strain. Although the notion of the polymer substrate delocalizing the strain in the metal film is appealing, both from practical and theoretical point of view, we caution that we are unaware of definitive experiments that fully confirm this notion. The rupture-debond co-evolution has not yet been convincingly demonstrated experimentally. The process poses an interesting computational problem. Different polymer substrates and a wide range of film/substrate thickness ratio have been used in practice. The effects of substrate strength and thickness on strain delocalization in metal films should be studied.

Acknowledgments

The work was supported by the New Jersey Commission of Science and Technology, by the National Science Foundation through the MRSEC at Princeton University, and by the Division of Engineering and Applied Sciences at Harvard University. TL also acknowledges the support of the Princeton Materials Institute Fellowship. The authors are grateful to J.W. Hutchinson and J.J. Vlassak for discussions and written comments on the paper.

References

Alaca, B.E., Saif, M.T.A., Sehitoglu, H., 2002. On the interface debond at the edge of a thin film on a thick substrate. Acta Mater. 50, 1197–1209.

Baker, S.P., Zhang, L., Gao, H., 2002. Effect of dislocation core spreading at interfaces on strength of thin-films. J. Mater. Res. 17, 1080–1813.

Baral, D., Ketterson, J.B., Milliard, J.E., 1984. Mechanical properties of composition modulated Cu-Ni foils. J. Appl. Phys. 57, 1076–1083.

Bigoni, D., Ortiz, M., Needleman, A., 1997. Effect of interfacial compliance on bifurcation of a layer bonded to a substrate. Int. J. Solids Struct. 34, 4305–4326.

Chiu, S.L., Leu, J., Ho, P.S., 1994. Fracture of metal–polymer line structures. I. Semiflexible polyimide. J. Appl. Phys. 76, 5136–5142.

Dorris, J.F., Nemat-Nasser, S., 1980. Instability of a layer on a half space. J. Appl. Mech. 47, 304–312.

Espinosa, H.D., Prorok, B.C., Fischer, M., 2003. A methodology for determining mechanical properties of freestanding films and MEMS materials. J. Mech. Phys. Solids 51, 47–67.

Gage, D.M., Phanitsiri, M., 2001. Experimental and mathematical analysis of tensile fracture mechanics in thin-film metal deposits, Senior Thesis, Princeton University.

Gleskova, H., Wagner, S., Suo, Z., 1999. Stability of amorphous silicon transistors under extreme in-plane strain. Appl. Phys. Lett. 75, 3011–3013.

Hill, R., Hutchinson, J.W., 1975. Bifurcation phenomena in the plane tension test. J. Mech. Phys. Solids 23, 239–264.

Hommel, M., Kraft, O., 2001. Deformation behavior of thin copper films on deformable substrates. Acta Mater. 49, 3935–3947.

Hsu, P.-H., Bhattacharya, R., Gleskova, H., Xi, Z., Suo, Z., Wagner, S., Sturm, J.C., 2002. Thin-film transistor circuits on large-area spherical surfaces. Appl. Phys. Lett. 81, 1723–1725.

Huang, H., Spaepen, F., 2000. Tensile testing of free-standing Cu, Ag and Al thin films and Ag/Cu multilayers. Acta Mater. 48, 3261–3269.

Hutchinson, J.W., Suo, Z., 1992. Mixed-mode cracking in layered materials, 1991. Adv. Appl. Mech. 29, 63–191.

Kang, Y.-S., 1996. Microstructure and strengthening mechanisms in aluminum thin films on polyimide film, Ph.D. Thesis, supervised by P.H. Ho, The University of Texas at Austin.

Keller, R.R., Phelps, J.M., Read, D.T., 1996. Tensile and fracture behavior of free-standing copper films. Mater. Sci. and Eng. A 214, 42–52.

Kraft, O., Hommel, M., Arzt, E., 2000. X-ray diffraction as a tool to study the mechanical behavior of thin films. Mater. Sci. Eng. A 288, 209–216.

Lacour, S.P., Wagner, S., Huang, Z.Y., Suo, Z., 2003. Stretchable gold conductors on elastomeric substrates. Appl. Phys. Lett. 82, 2404–2406.

Lee, H.J., Zhang, P., Bravman, J.C., 2003. Tensile failure by grain thinning in micromachined aluminum thin film. J. Appl. Phys. 93, 1443–1451.

Lumelsky, V.J., Shur, M.S., Wagner, S., 2001. Sensitive skin. IEEE Sensors J. 1, 41–51.

Merchant, H.D., Wang, J.T., Giannuzzi, L.A., Liu, Y.L., 2000. Metallurgy and performance of electrodeposited copper for flexible circuits. Circuit World 26 (4), 7–14.

Nicola, L., Van der Giessen, E., Needleman, A., 2003. Discrete dislocation analysis of size effects in thin films. J. Appl. Phys. 93, 5920–5928.

Nix, W.D., 1998. Yielding and strain hardening of thin metal films on substrates. Scripta Mater. 39, 545–554.

Pashley, D.W., 1960. A study of the deformation and fracture of single-crystal gold films of high strength inside an electron microscope. Proc. Roy. Soc. Lond. A 255, 218–231.

Steif, P.P., 1986. Periodic necking instabilities in layered plastic solids. Int. J. Solids Struct. 22, 195–207.

Stören, S., Rice, J.R., 1975. Localized necking in thin sheets. J. Mech. Phys. Solids. 23, 421–441.

Tvergaard, V., Needleman, A., Lo, K.K., 1981. Flow localization in the plane strain tensile test. J. Mech. Phys. Solids 29, 115–142.

Wagner, S., Bonderover, E., Jordan, W.B., Sturm, J.C., 2002. Electrotextiles: concepts and challenges. Int. J. High Speed Electron. Syst. 12, 1–9.

Xiang, Y., Chen, X., Vlassak, J.J., 2002. The mechanical properties of electroplated Cu thin films measured by means of the bulge test techniques. Mater. Res. Soc. Symp. Proc. 695, L4.9.

Yu, D.Y.W., Spaepen, F., 2004. The yield strength of thin copper films on Kapton. J. Appl. Phys. 95 (6), 2991–2997.